

Σ
SPE 49266

Modeling Relative Permeability Effects in Gas-Condensate Reservoirs

G.A. Pope, W. Wu, G. Narayanaswamy, M. Delshad, M. Sharma, P. Wang

Department of Petroleum and Geosystems Engineering, The University of Texas at Austin

Copyright 1998, Society of Petroleum Engineers, Inc.

This paper was prepared for presentation at the 1998 SPE Annual Technical Conference and Exhibition held in New Orleans, Louisiana, 27–30 September 1998.

This paper was selected for presentation by an SPE Program Committee following review of information contained in an abstract submitted by the author(s). Contents of the paper, as presented, have not been reviewed by the Society of Petroleum Engineers and are subject to correction by the author(s). The material, as presented, does not necessarily reflect any position of the Society of Petroleum Engineers, its officers, or members. Papers presented at SPE meetings are subject to publication review by Editorial Committees of the Society of Petroleum Engineers. Electronic reproduction, distribution, or storage of any part of this paper for commercial purposes without the written consent of the Society of Petroleum Engineers is prohibited. Permission to reproduce in print is restricted to an abstract of not more than 300 words; illustrations may not be copied. The abstract must contain conspicuous acknowledgment of where and by whom the paper was presented. Write Librarian, SPE, P.O. Box 833836, Richardson, TX 75083-3836, U.S.A., fax 01-972-952-9435.

Abstract

Many gas condensate wells show a significant decrease in productivity once the pressure falls below the dew point pressure. This significantly decreases the productivity of very high rate gas wells in many of the world's largest hydrocarbon reservoirs. A widely accepted cause of this decrease in productivity index (PI) is the decrease in gas relative permeability due to build up of condensate in the near wellbore region. Predictions of well inflow performance require accurate models for the gas relative permeability as a function of interfacial tension (IFT) between the gas and condensate phases (actually it should be trapping number rather than IFT). Since these relative permeabilities depend on fluid composition and pressure as well as condensate and water saturations, a model is essential for both interpretation of lab data and for predictive field simulations. The key to such a gas condensate relative permeability model is the dependence of the critical condensate saturation on the capillary number or its generalization called the trapping number. We have made careful comparisons of such data with a capillary trapping model and have found that we can match these data with a simple two-parameter model. We then developed a general

scheme for computing the gas and condensate relative permeabilities as a function of the capillary trapping model and with only data at low trapping number (high IFT) as input and have found good agreement with the experimental data in the literature. We then used this model and typical parameters for gas condensates in a compositional simulation study of a single well to better understand the PI behavior of the well and the significance of the condensate buildup.

Introduction

Afidick *et al.*¹ and Barnum *et al.*² have reported field data which show that under some conditions significant loss of well productivity can occur in some gas wells due to near wellbore condensate accumulation. As pointed out by Boom *et al.*,³ even for lean fluids with very low condensate dropout, high condensate saturations may build up as many pore volumes of gas pass through the near wellbore region. As the condensate saturation increases, the gas relative permeability decreases and thus the productivity of the well decreases. The gas relative permeability is a function of the interfacial tension between the gas and condensate among other variables. For this reason, several laboratory studies³⁻¹⁴ have been reported on the measurement of relative permeabilities of gas condensate fluids as a function of interfacial tension. These studies show a significant increase in the relative permeability of the gas as the interfacial tension between the gas and condensate decreases. The relative permeabilities of the gas and condensate have often been modeled directly as an empirical function of the interfacial tension.¹⁵ However, it has been known since at least 1949¹⁶ that the relative permeabilities in general actually depend on the ratio of forces on the trapped phase, which can be expressed as either a capillary number or

Bond number. This has been recognized in recent years to be true for gas condensate relative permeabilities.^{8,10} Below we describe a model for correlating relative permeabilities as a function of a new trapping number which is more general than any model in the literature but is still easy to use, requires a minimum of experimental data, and has been found to agree well with a variety of experimental data. This model is a generalization of the approach first presented by Delshad *et al.*¹⁷ As shown below, this relative permeability model agrees well with gas condensate data from the literature. We then show simulations of a gas condensate well to illustrate the effect of condensate buildup on the well productivity with and without the capillary number effect.

Model Description

The fundamental problem with condensate buildup in the reservoir is that capillary forces can retain the condensate in the pores unless the forces displacing the condensate exceed the capillary forces. To the degree that the pressure forces in the displacing gas phase and the buoyancy force on the condensate exceed the capillary force on the condensate, the condensate saturation will be reduced and the gas relative permeability increased. This problem is analogous to the trapping of oil by water during a waterflood in which case it is loosely referred to as residual oil saturation and has been studied for decades. Brownell and Katz¹⁶ and others recognized early on that the residual oil saturation should be a function of the ratio of viscous to interfacial forces and defined a capillary number to capture this ratio. Since then many variations on the definition have been published¹⁷⁻²⁰ with some of the most common ones written in terms of the velocity of the displacing fluid, which can be done by using Darcy's law to replace the pressure gradient with velocity. However, it is the force on the trapped fluid that is most fundamental and so we prefer the following definition:

$$N_{c\ell} = \frac{|\vec{k} \cdot \vec{\nabla} \Phi_{\ell'}|}{\sigma_{\ell\ell'}} \quad (1)$$

where the gradient of the flow potential is given by $\vec{\nabla} \Phi_{\ell'} = \vec{\nabla} P_{\ell'} - g\rho_{\ell'} \vec{D}$. Although the distinction is not usually made, one should designate the displacing phase ℓ' and the displaced phase ℓ in any such definition. In some cases, buoyancy forces can contribute significantly to the total force on the trapped phase. To quantify this effect, the Bond number was introduced and also takes different forms in the literature.²⁰ One such definition is as follows:

$$N_{B\ell} = \frac{k g (\rho_{\ell'} - \rho_{\ell})}{\sigma_{\ell\ell'}} \quad (2)$$

For special cases such as vertical flow, the force vectors are collinear and one can just add the scalar values of the viscous and buoyancy forces and correlate the residual oil saturation with the this sum, or in some cases one force is negligible compared to the other force and just the capillary number or Bond number can be used by themselves. This is the case with most laboratory studies including the recent ones by Boom *et al.*^{3,8} and Henderson *et al.*¹⁰ However, in general the forces on the trapped phase are not collinear in reservoir flow and the vector sum must be used. In fact, the viscous forces are most often nearly horizontal and the buoyancy force is vertical, so a scalar sum is completely wrong. A generalization of the capillary and Bond numbers was derived by Jin²¹ and called the trapping number. The trapping number for phase ℓ displaced by phase ℓ' is defined as follows:

$$N_{T\ell} = \frac{|\vec{k} \cdot (\vec{\nabla} \Phi_{\ell'} + g\Delta\rho \vec{D})|}{\sigma_{\ell\ell'}} \quad (3)$$

This definition does not explicitly account for the very important effects of spreading and wetting on the trapping of a residual phase. However, it does an excellent job of correlating the residual saturation of both a wide variety of phases of differing wettabilities and a wide variety of rock types, so it is very useful for modeling a particular set of rock and fluid conditions if a few basic data have been measured to establish the correlation.

The residual saturation is modeled based on the trapping number as shown below.

$$S_{\ell r} = \min \left(S_{\ell}, S_{\ell r}^{\text{high}} + \frac{S_{\ell r}^{\text{low}} - S_{\ell r}^{\text{high}}}{1 + T_{\ell} (N_{T\ell})^{\tau_{\ell}}} \right) \quad (4)$$

In the above equation, $S_{\ell r}$ is the residual saturation for phase ℓ and S_{ℓ} is the saturation of phase ℓ . The superscripts high and low refer to high and low trapping numbers. $S_{\ell r}^{\text{high}}$ is typically zero. The trapping parameters T_{ℓ} and τ_{ℓ} are obtained by fitting residual saturation data for phase ℓ . τ_{ℓ} is typically 1.0, however, some of the condensate data from the literature can be fit somewhat better by using τ_{ℓ} as a second fitting

parameter. Mass transfer can reduce the value of S_ℓ to values less than $S_{\ell r}$ which is the reason why the minimum is taken in Eq. (4). For example, dry gas flowing by residual condensate at a fixed pressure can strip the lighter components from the condensate and reduce its saturation.

Establishing the correlation of residual saturations with the trapping number (or special cases of it as appropriate) is the first and most fundamental step in correlating relative permeability data as a function of interfacial tension. Although we have always found Eq. (4) to be adequate and convenient for this purpose for a wide variety of data sets including gas condensates, a table could also be used to represent the decrease in residual saturations with increasing trapping number, or for that matter some other simple function that fits the data. In cases such as gas condensates there are three residual phases (gas, condensate, and water) and this correlation has been found to apply to all three phases.

The next step is to correlate the endpoint relative permeability of each phase, which increases in a very predictable way as the trapping number increases and can be correlated using the following equation.

$$k_{r\ell}^o = k_{r\ell}^{o \text{ low}} + \frac{S_{\ell r}^{\text{low}} - S_{\ell r}}{S_{\ell r}^{\text{low}} - S_{\ell r}^{\text{high}}} (k_{r\ell}^{o \text{ high}} - k_{r\ell}^{o \text{ low}}) \quad (5)$$

where $S_{\ell r}$ is the residual saturation of the conjugate phase e.g. condensate is the conjugate phase for gas. This equation has also been found to provide a good correlation of a wide variety of data. The final step is to calculate the relative permeability of each phase ℓ as a function of saturation. One approach to this problem is to assume a simple function such as a Corey-type relative permeability function.¹⁷ This then requires correlating the Corey exponent with trapping number. Equation (5) written in terms of the exponent rather than the endpoint can be used for this purpose.²² However, not all relative permeability data can be fit with a Corey-type model, so we have generalized our approach by using the following equation:

$$\log k_{r\ell} = \log k_{r\ell}^o + \log \bar{S}_\ell + \frac{\log \left(\frac{k_{r\ell}}{k_{r\ell}^o} \right)^{\text{low}} - \log \bar{S}_\ell}{1 + T_\ell (N_{T_\ell})^{\tau_\ell}} \quad (6)$$

where $k_{r\ell}$ is the relative permeability and $k_{r\ell}^o$ is the endpoint relative permeability for a given trapping number and saturation. $k_{r\ell}^{\text{low}}$ and $k_{r\ell}^{o \text{ low}}$ are the relative permeability and endpoint relative permeability at a low trapping number for phase ℓ .

The normalized saturations (\bar{S}_ℓ) in the above equation are defined as

$$\bar{S}_\ell = \frac{S_\ell - S_{\ell r}}{1 - \sum_{\ell=1}^{n_p} S_{\ell r}} \quad (7)$$

where n_p is the number of phases present, S_ℓ is the saturation and $S_{\ell r}$ is the residual saturation for phase ℓ , which are calculated using equation (4).

Only the baseline relative permeability curve of each phase at low trapping number corresponding to the usual laboratory measurements and the residual saturations as a function of the trapping number are needed in this approach. Figures 1 and 2 show the computed relative permeability of gas and condensate calculated for a wide range of trapping numbers using just two parameters. Although this model captures the general trends in the data very well, there are still some issues such as hysteresis which have not been adequately investigated for gas condensates. However, it should be a great improvement over the traditional approach used in compositional reservoir simulators that are used to model gas condensate reservoirs.

Comparisons With Experimental Data

As pointed out above, the best starting point for understanding and modeling relative permeability data as a function of interfacial tension is the relationship between the residual saturations and trapping number (or its special cases of capillary number or Bond number when appropriate to the experimental conditions). For this reason, we first show an example of normalized residual saturations versus trapping number in Figure 3. The residual saturations were normalized by dividing them by the low trapping number plateau values. As seen from these data, there is a very large difference between the nonwetting and wetting phase data. A much larger trapping number is required to decrease the residual saturation for the wetting phase than for the nonwetting phase. This is typical of all of the data in the literature for all types of phases and rocks (e.g. see the review in Delshad²²). We selected these data from the many examples in the literature to make the point that even widely different phases have similar behavior in a given rock if their wettability is the same. The

nonwetting phases in Fig. 3 are the gas and oil. The gas data from Henderson *et al.*¹⁰ are for the equilibrium gas in a binary mixture of methane and n-butane intended to represent a gas condensate fluid. The oil data from Delshad²² are for the equilibrium oil for a mixture of decane, brine, isobutanol and sodium sulfonate under three-phase conditions. The wetting phases in Fig. 3 are the aqueous and microemulsion phases. The aqueous data from Boom *et al.*^{3,8} are for the equilibrium aqueous phase in a ternary mixture of water, n-heptane and isopropyl alcohol. The microemulsion data from Delshad²² are for the equilibrium microemulsion. The condensate data from Henderson *et al.*¹⁰ appear to be of intermediate wettability (between the gas and water), which emphasizes the importance including all three phases in the experiments.

More examples of wetting phase data for several different porous media are shown in Fig. 4. The corresponding data for the nonwetting phase are shown in Fig. 5. These data emphasize the strong dependence on the rock as well as the wettability of the phases. The strong conclusion is that one must measure the residual saturations for the wetting state and rock of interest to get useful results that can be accurately applied to a particular reservoir state. In particular, if there are three phases in the reservoir such as there are with gas condensates, then to ensure the correct wetting and spreading state in the rock, three phases need to be in the laboratory core even if one of the phases such as the brine is always at residual saturation. There are too many other similar examples in the literature to review here, but many other data can be found in Stegemeier,²³ Morrow and Chatzis²⁴ and Delshad²² among others. Stegemeier²³ provides an excellent theoretical treatment as well.

All of the data shown in Figs. 3 to 5 were fit using just one parameter T_ℓ for each phase ℓ and the value of this parameter is shown on each figure. Next we show the comparisons with endpoint relative permeabilities using these same values of T_ℓ . Figure 6 shows the endpoint relative permeability of the gas phase as a function of trapping number for the methane/n-butane binary mixture from both Hartman and Cullick⁷ and Henderson *et al.*¹⁰ Figure 7 shows the endpoint relative permeability for various liquid phases and porous media as a function of the trapping number. The values vary significantly due to the differing rocks and for the same rock such as Berea sandstone due to the differing wettability. However, the general trend of increasing endpoint relative permeability with increasing trapping number is consistent and clear and agrees with that previously reported by Delshad *et al.*¹⁷ for widely different fluids.

The curve calculated from Eq. (5) of the model is shown for comparison with these data. In all of these cases, the endpoint relative permeability appears to approach 1.0 at a

sufficiently high trapping number. This high trapping number value is sometimes referred to as the miscible value, but strictly speaking it is still an immiscible value even if the interfacial tension is ultralow. As shown in Delshad,²² the interfacial tension can be high and the trapping number still made high enough in the laboratory by increasing the pressure gradient to make the endpoint approach one, so it is not the interfacial tension that matters per se, but rather the trapping number. The endpoint relative permeability was not always measured by these investigators at a sufficiently low value of trapping number to determine its value directly, so its value had to be estimated by fitting the available data at intermediate trapping numbers. This value is often referred to as the immiscible value of the endpoint, but clearly this is not a useful designation. Its value depends on the value of the trapping number. In some cases, a plateau value of the endpoint at some sufficiently low trapping number is observed, but this is not always the case, especially for heterogeneous rocks and any phase that is wetting or even mixed wet. For these and other fundamental reasons, the designations of miscible and immiscible values are not correct or useful, nor is meaningful to describe these data in terms of high and low interfacial tension, but rather only in terms of high or low trapping number.

Figures 8 to 11 show comparisons between the model curves and several sets of relative permeability data for gas and condensate fluids. No new parameters were introduced and yet all of the trends in the data are captured reasonably well. The capillary numbers shown on Figs. 8 and 9 correspond to the definition used by Henderson *et al.*,¹⁰ which is based upon velocity rather than potential gradient. Since their experiments were done with their capillary number held constant, it made more sense to plot these relative permeability data using their definition. Under their experimental conditions, buoyancy was negligible, so our model could be used with either definition of capillary number. In general, however, the trapping number should be used.

It is important to note that very few parameters are needed in this model and that it goes to all of the correct limits observed not just for these data but for other literature data for various cores, fluids and conditions. Our modeling efforts show that for reasonable prediction of relative permeability at various trapping numbers, the measurement of endpoint relative permeabilities at different trapping numbers is more important than the measurement of relative permeabilities at various saturations at different trapping numbers. It is our hope that future experimental studies will show more emphasis on measuring endpoint relative permeabilities.

Numerical Simulations

We used the relative permeability curves of Figs. 1 and 2 to investigate the effect of trapping number on the productivity of a single well in a gas condensate reservoir. The equation-of-state (EOS) compositional reservoir simulator UTCOMP was used in this study.²⁵ The fluid description and phase behavior is the same as given in Wu *et al.*²⁶ using the approach of Wang *et al.*²⁷ to accurately model the behavior of a gas condensate fluid using six hydrocarbon components. For simplicity, a layered-permeability description was used for this initial simulation study. Both the reservoir description and phase behavior are similar to those of the Arun field studied by Afidick *et al.*¹ However, these simulations are not meant to apply to the Arun field, but rather were done simply to illustrate the trends in the PI with trapping number. A systematic simulation study of the Arun field including a history match of PI can be found in Narayanaswamy.²⁸

Description of Simulation Data

The simulation domain used was a two-dimensional vertical cross-section (x-z) with a fan shape at an angle of 36° (Figure 12). The simulation grid has 8 layers (Table 1) with the highest permeability layer at the top (90 md) and the lowest permeability layer at the bottom (1.5 md). Nineteen gridblocks were used in the x direction with a variable gridblock size of 1 to 500 ft and with the smaller gridblocks located near the wellbore. The well is producing at a constant rate of 4.4×10^6 SCF/D (corresponds to one-tenth of the full well rate) and it penetrates all 8 layers. A constant pressure (4100 psia) boundary condition was applied to the outer boundary of the fan-shaped reservoir, which allows fluid with the initial composition to flow into the simulation domain. The reservoir temperature and pressure are 335 °F and 4100 psia, so the initial fluid composition is in the two-phase region.

Discussion of Results

We performed simulations with and without the effects of trapping number on the relative permeability to demonstrate its significance on condensate saturation and productivity index (PI). Figures 13 and 14 illustrate the distribution of condensate with and without the effect of trapping number. Figure 13 shows that the condensate saturation goes through a maximum in the high permeability layers with distance from the well. This is because the trapping number results in low values of condensate very close to the well in the high permeability layers, then the condensate saturation increases as the trapping number decreases with increasing distance from

the well, and it finally decreases again due to the increase in the pressure. The maximum condensate saturation occurs farther away from wellbore in the top (high permeability) layers. Figure 14 shows the condensate saturation in the near wellbore region for the case without trapping number modeled is high near the well and then decreases away from the well in all layers.

Figure 15 illustrates the range of the trapping numbers encountered in both the top and bottom layers for the simulation as a function of distance from the wellbore. In the top layer, trapping numbers are above the critical trapping number (about 10^{-6} from Fig. 3) for up to the 100 ft from the wellbore. In the bottom layer that has the lowest permeability, no increase in relative permeability due to trapping number effects will be seen because the trapping number is less than the critical trapping number.

Figures 16 shows the condensate saturation in layer 1 as a function of distance from the well with and without trapping number modeled and for two values of endpoint gas relative permeability. The variations in condensate saturation are more significant with the lower endpoint gas relative permeability. The use of 0.2 as the endpoint gas relative permeability enlarges the range of relative permeabilities and hence more significant effects of the trapping number are observed.

The normalized well productivity index, with and without trapping number and for two different gas endpoints, is shown in Fig. 17 as a function of the average reservoir pressure. The productivity index (PI) in this study was computed using the following equation:

$$PI = \frac{Q}{P_{ave} - P_{wf}} \quad (8)$$

where Q is total production rate in MMSCF/D, P_{ave} is the average reservoir pressure in psia and P_{wf} is bottomhole flowing pressure from the top layer in psia. The ratio of the PI to the initial PI gives the normalized PI. The initial productivity index was taken at time 0.01 days for each case.

Figure 17 shows that the PI decreases rapidly as condensate builds up in the reservoir, but that the effect is somewhat attenuated when the reduction in condensate saturation at high values of trapping number is modeled. The trapping number effect is more significant for the case of low endpoint gas relative permeability than for the higher value. After a certain period of production, the difference in the productivity between these two runs becomes almost unchanged: the run with the trapping number effects remains around 35% higher productivity for the case with an endpoint of 0.53. The productivity modeled with trapping number is

approximately twice the productivity without trapping number when using the low endpoint gas curve (0.2). Table 2 lists the productivity index for the partial well in each layer with and without trapping number effects after 10 days of production. The layer-averaged pressure and bottomhole pressure at each layer were used for the P_{ave} and P_{wf} in Eq. (8). It can be seen from Table 2 that the productivity index is more than two times greater in the top two layers when trapping number effects are modeled. The productivity index decreases as the formation permeability decreases. In the bottom two layers, no significant effects of the trapping number on the productivity index were observed.

This simulation study shows why relative permeability should not be modeled based on IFT only. The fundamental nature of changes in relative permeability has been shown using the trapping number concept. The basic equations clearly indicate that IFT is not the only factor affecting residual saturations and the critical condensate saturation in particular. Hence, the crucial rate effects which contribute significantly in the near wellbore region will not be accounted for by an IFT model. The reduction in condensate saturation in high permeability layers near the wellbore will not be shown by such a model. Conditions in the near wellbore region for high permeability layers are the most important factors affecting the PI. Hence, relative permeability models based on IFT only have a very poor chance of making accurate predictions of PI. Furthermore, it would be very difficult to model all of these interacting effects analytically since heterogeneity, pressure, phase behavior, interfacial tension, trapping number and relative permeability are all coupled in a complex and nonlinear way. The coupling with heterogeneity is strong even when the reservoir description is very simple as in this example. We are currently using stochastically generated permeability fields to further elucidate this coupling for more realistic reservoir descriptions.²⁸ Assuming a uniform condensate buildup close to the wellbore is not correct and does not lead to accurate predictions, nor is it reasonable to assume a donut shaped condensate bank near the wellbore.

In addition, for simplicity and clarity, we did not include non-Darcy effects in this illustrative simulation, but for very high rate gas wells, non-Darcy flow can be significant and is also coupled with all of the above variables and should be taken into account.²⁸⁻³⁰

Summary And Conclusions

The buildup of condensate close to gas condensate wells can significantly reduce the gas relative permeability and thus the PI of the well and must be accounted for with an accurate relative permeability model. Although interfacial tension can

be low and variable and does effect the gas and condensate relative permeabilities, it is not correct or accurate to model the relative permeabilities directly as a function of interfacial tension, but rather they should be modeled as a function of the combined effects of pressure gradient, buoyancy and capillary forces. This requires a generalization of the classical capillary number and Bond number into a trapping number. As shown in this paper, this trapping number can be used in a generalized relative permeability model to correlate gas condensate data and then used in a simulator to predict changes in PI due to changes in condensate saturation.

Acknowledgments

We thank Mobil for funding this research project and specifically thank the members of the gas condensate team at Mobil Exploration and Production Technical Center (Meptec): Kathy Hartman, Myung Hwang, Ravi Vaidya, Jim Dixon, Steve Weber and Mary Coles for useful discussions and suggestions during the course of this research. We also wish to thank Rene Frederiksen for his help with some of the model calculations.

References

1. Afidick, D., N.J. Kaczorowski, and S. Bette: "Production Performance of a Retrograde Gas: A Case Study of the Arun field," *paper SPE 28749* presented at the Asia Pacific Oil & Gas Conference, Melbourne, Australia, Nov. 7-10, 1994.
2. Barnum, R.S., F.P. Brinkman, T.W. Richardson and A.G. Spillette: "Gas Condensate Reservoir Behavior: Productivity and Recovery Reduction Due to Condensation," *paper SPE 30767* presented at the SPE Annual Technical Conference & Exhibition held in Dallas, Texas, Oct. 22-25, 1995.
3. Boom, W., K. Wit, J.P.W. Zeelenberg, H.C. Weeda, and J.G. Maas: "On the Use of Model Experiments for Assessing Improved Gas-Condensate Mobility Under Near-Wellbore Flow Conditions," *paper SPE 36714* presented at the SPE Annual Technical Conference and Exhibition held at Denver, Colorado, Oct. 6-9, 1996.
4. Asar, H and L.L. Handy: "Influence of Interfacial Tension on Gas/Oil Relative Permeability in a Gas-Condensate System," *SPERE* (Feb. 1988) 257-264.
5. Hanif, M.S. and J.K. Ali: "Relative Permeability and Low Tension Fluid Flow in Gas Condensate Systems," *paper SPE 20917* presented at the European Petroleum Conference held in The Hague, Netherlands, Oct. 22-24 1990.
6. Bardon, C. and D.G. Longeron: "Influence of Very Low Interfacial Tensions on Relative Permeability," *SPEJ* (Oct. 1980), 391-401.
7. Hartman, K.J. and A.S. Cullick: "Oil Recovery by Gas Displacement at Low Interfacial Tension," *J. Pet. Sci. and Eng.* 10 (1994) 197-210.
8. Boom, W., K. Wit, A.M. Schulte, S. Oedai, J.P.W. Zeelenberg, and J.G. Maas: "Experimental Evidence for Improved Condensate Mobility at Near-wellbore Flow Conditions," *paper SPE 30766* presented at the SPE Annual Technical Conference and Exhibition, Dallas Texas, Oct. 22-25, 1995.

9. Chen, H.L., T.G. Monger-McClure, S.D. Wilson: "Determination of Relative Permeability and Recovery for North Sea Gas Condensate Reservoirs," paper SPE 30769 presented at the SPE Annual Technical Conference & Exhibition, Dallas, Texas, October 22-25, 1995.
10. Henderson, G.D., A. Danesh, D.H. Tehrani, S. Al-Shaidi, and J.M. Peden: "Measurement and Correlation of Gas Condensate Relative Permeability by the Steady-State Method," *SPEJ* (Jan. 1996).
11. Kalaydjian, F.J.M., B.J. Bourbiaux and J.M. Lombard: "Predicting gas-condensate reservoir performance: how flow parameters are altered when approaching production wells," SPE 36715 presented at the SPE Annual Technical Conference, Denver, Colorado, Oct. 6-9 1996.
12. Ali, J.K., P.J. McGauley and C.J. Wilson: "The Effects of High-Velocity Flow and PVT Changes Near the Wellbore on Condensate Well Performance," paper SPE 38923 presented at the SPE Annual Technical Conference and Exhibition held in San Antonio, Texas, October 5-8, 1997.
13. Morel, D.C., A. Nectoux and J. Danquigny: "Experimental Determination of the Mobility of Hydrocarbon Liquids during Gas Condensate Reservoir Depletion: Three Actual Cases," paper SPE 38922 presented at the SPE Annual Technical Conference and Exhibition, San Antonio, Texas, October 5-8, 1997.
14. McDougall, S. R., P.A. Salino and K. S. Sorbie: "The Effect of Interfacial Tension Upon Gas-Oil Relative Permeability Measurements: Interpretation Using Pore-Scale Models," paper SPE 38920 presented at the SPE Annual Technical Conference and Exhibition, San Antonio, Texas, October 5-8, 1997.
15. Coats, K.H.: "An Equation of State Compositional Model," *SPEJ*, 20 (1980) 363-376.
16. Brownell, L.E. and D.L. Katz: "Flow of Fluids through Porous Media," *Chem. Eng. Pros.*, 43 (1949) 601-612.
17. Delshad M., M. Delshad, D. Bhuyan, G.A. Pope and L.W. Lake: "Effects of Capillary Number on the Residual Saturation of Three Phase Micellar Solution," paper SPE 14911 Proceedings of the SPE/DOE 5th Symposium on Enhanced Oil Recovery, Tulsa, Oklahoma, Apr. 20-23, 1986.
18. Lake, L.W.: "*Enhanced Oil Recovery*," Prentice-Hall, Englewood Cliff, New Jersey, (1989).
19. Jerauld, G.R.: "General Three-phase Relative Permeability Model for Prudhoe Bay," *SPERE*, (Nov. 1997) 255-263.
20. Morrow, N.R. and B. Songkran: "Surface Phenomena in Enhanced Oil Recovery," D. O. Shah (ed.), Plenum Press, New York City, (1982) 387-411.
21. Jin, Minquan: "A study of Non-Aqueous Phase Liquid Characterization and Surfactant Remediation," Ph.D. Dissertation, U. of Texas, Austin, 1995.
22. Delshad M.: "Trapping of Micellar Fluids in Berea Sandstone," Ph.D. dissertation, The U. of Texas, Austin, 1990.
23. Stegemeier, G.L.: "Mechanisms of Entrapment and Mobilization of Oil in Porous Media," Improved Oil Recovery by Surfactant and Polymer Flooding, Shah, D. O. and R. S. Schechter (eds.), Academic Press, New York City (1977) 55-91.
24. Chatzis, I. and N.R. Morrow: "Correlation of Capillary Number Relationships for Sandstones," paper SPE 10114 presented at the 56th Annual Conference of the SPE, San Antonio, Texas, Oct. 5-7, 1981.
25. Chang, Yih-Bor., G.A. Pope and K. Sepehrnoori: "A higher-order finite-difference compositional simulator," *Journal of Petroleum Science and Engineering*, 5 (1990) 35-50.
26. Wu, Wei-Jr, P. Wang, M. Delshad, C. Wang, G.A. Pope and M. Sharma: "Modeling Non-Equilibrium Mass Transfer Effects for a Gas Condensate Field," paper SPE 39746 presented at the Asia Pacific Conference held in Kuala Lumpur, Malaysia, March 23-24, 1998.
27. Wang, P., G.A. Pope and K. Sepehrnoori: "Development of Equations of State for Gas Condensates for Compositional Petroleum Reservoir Simulation," Submitted to Industrial & Engineering Chemistry Research, Nov. 1997.
28. Narayanaswamy, G: "Well Deliverability of Gas Condensate Reservoirs," M.S. Thesis, U. of Texas, Austin, 1998.
29. Blom, S. M. P and Hagoort, J.: "The Combined Effect of Near-Critical Relative Permeability and Non-Darcy Flow on Well Impairment by Condensate Drop-Out," paper SPE 39976 presented at the SPE Gas Technology Symposium, Calgary, Alberta, Canada, March 15-18, 1998.
30. Narayanaswamy, G., M. M. Sharma and G.A. Pope: "Effect of Heterogeneity on the Non-Darcy Flow Coefficient," paper SPE 39979 presented at the SPE Gas Technology Symposium, Calgary, Alberta, Canada, March 15-18, 1998.

Table 1—Reservoir Description			
Layer	Thickness (ft)	Porosity (fraction)	Permeability (md)
1	10	0.300	90
2	10	0.250	75
3	30	0.214	50
4	50	0.220	28
5	100	0.209	12
6	50	0.219	17
7	150	0.127	2.6
8	370	0.120	1.5

Table 2—Productivity Index (MSCFD/pai)			
Layer	$K_{rg}^* = 0.53$		$K_{rg}^* = 0.2$
	With N_T	Without N_T	Without N_T
1	16.486	8.244	2.825
2	13.120	6.868	2.353
3	23.739	13.732	4.779
4	20.008	12.801	4.895
5	16.300	13.120	4.358
6	12.931	8.482	6.446
7	4.839	5.705	1.856
8	7.433	7.933	3.346
			2.780

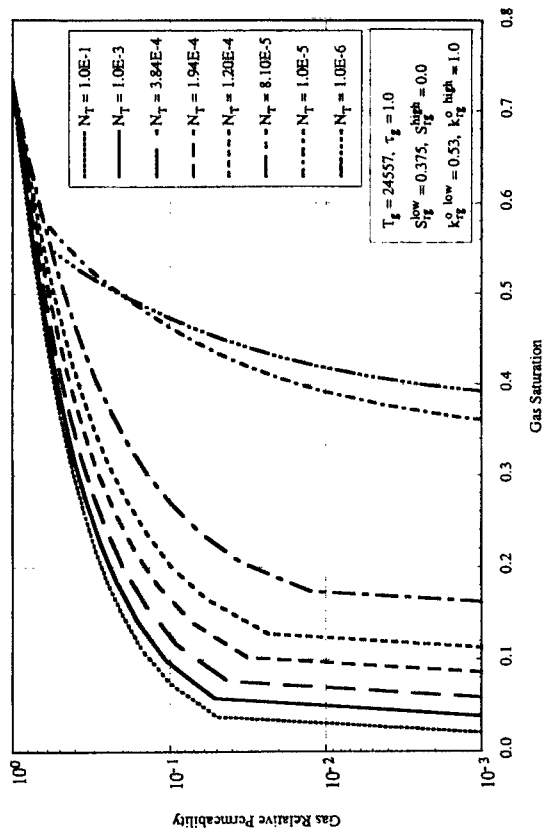


Fig. 1—Gas relative permeabilities calculated from trapping number model.

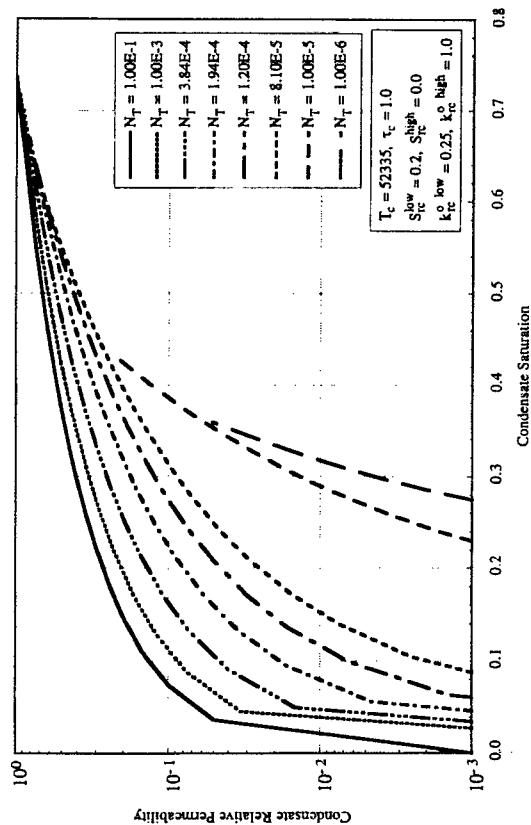


Fig. 2—Condensate relative permeabilities calculated from trapping number model.

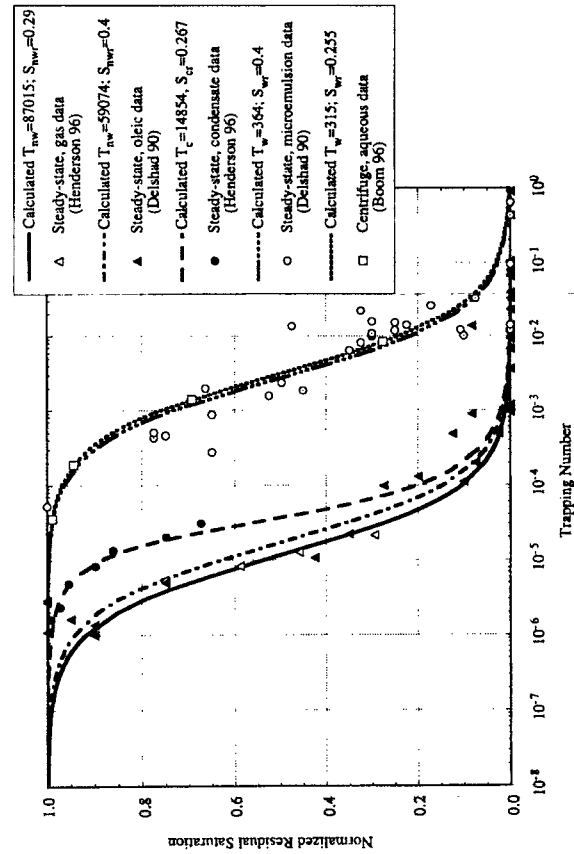


Fig. 3—Effect of wettability on the desaturation curves for Berea sandstone.

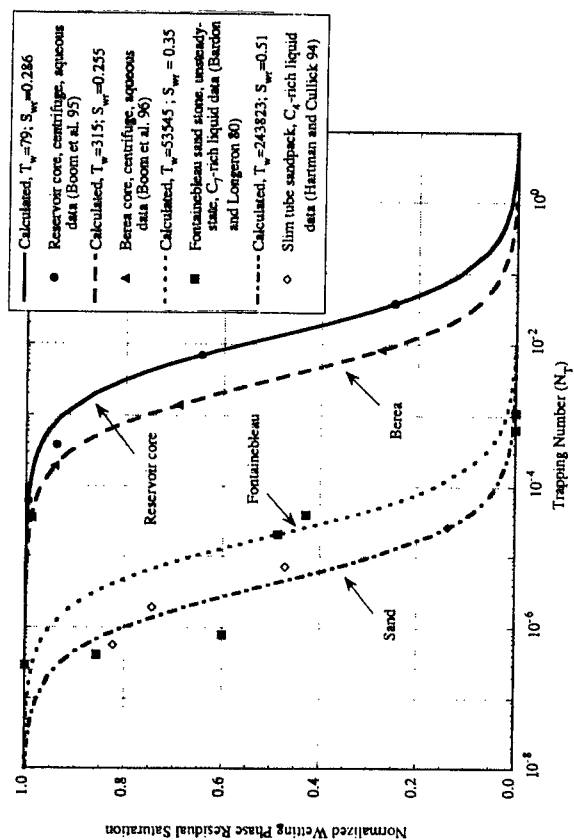


Fig. 4—Comparison of model with experimental wetting phase residual saturation data for various porous media.

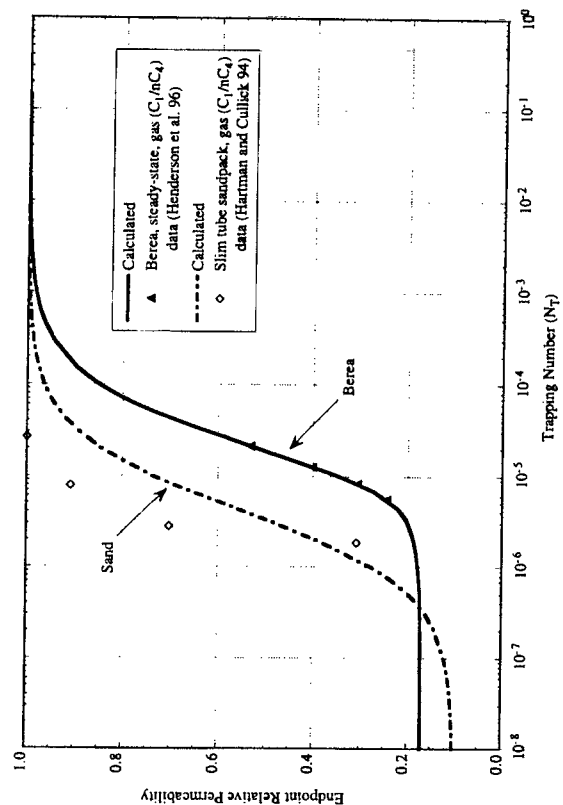


Fig. 5—Comparison of model with experimental nonwetting phase residual saturation data for various porous media.

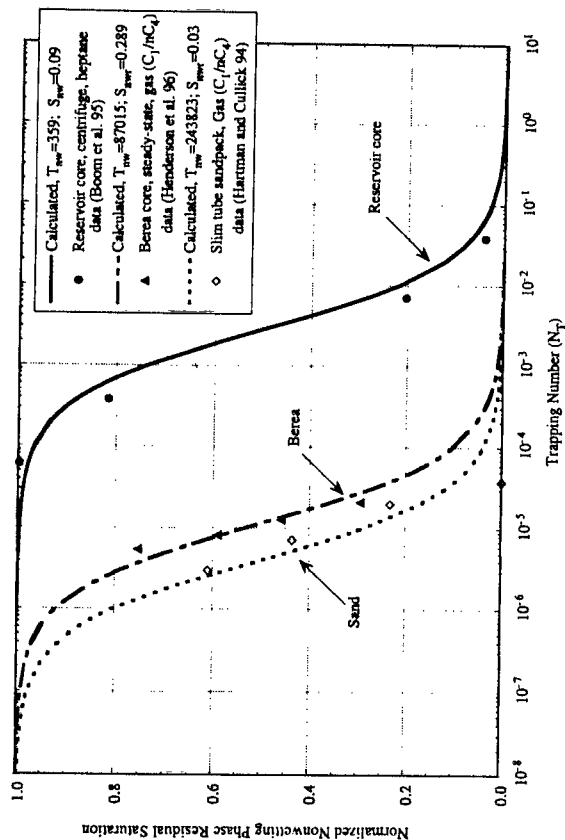


Fig. 6—Comparison of model with experimental wetting phase endpoint relative permeability data for various porous media.

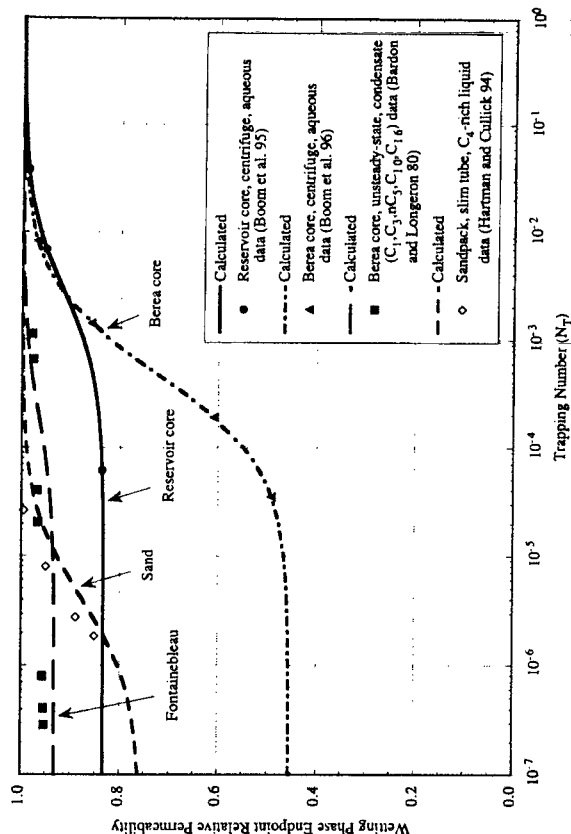


Fig. 7—Comparison of model with experimental nonwetting phase residual saturation data for various porous media.

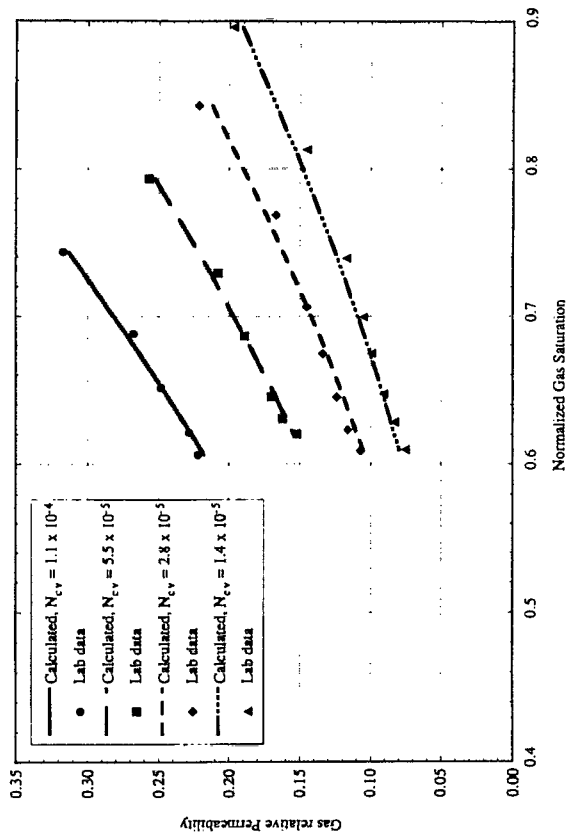


Fig. 8—Comparison of calculated and experimental gas relative permeability data (Henderson et al., 1996).

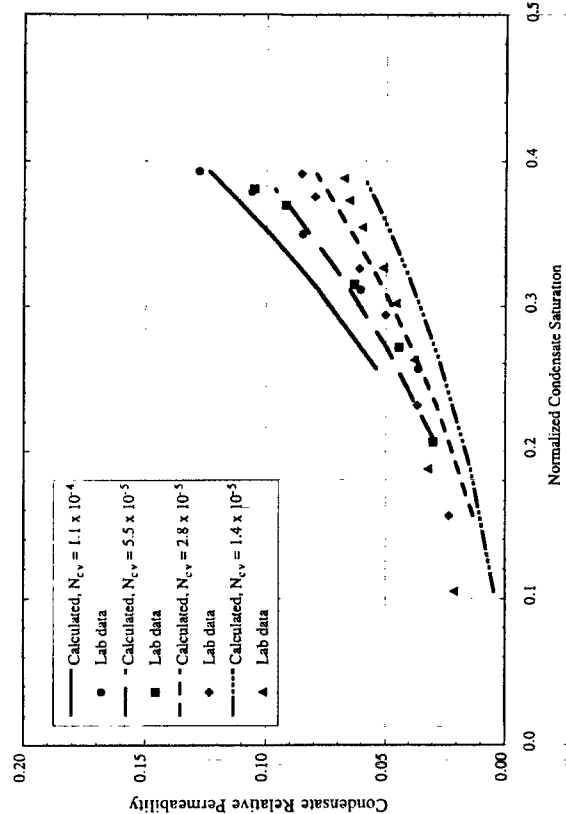


Fig. 9—Comparison of calculated and experimental condensate relative permeability data (Henderson et al., 1996).

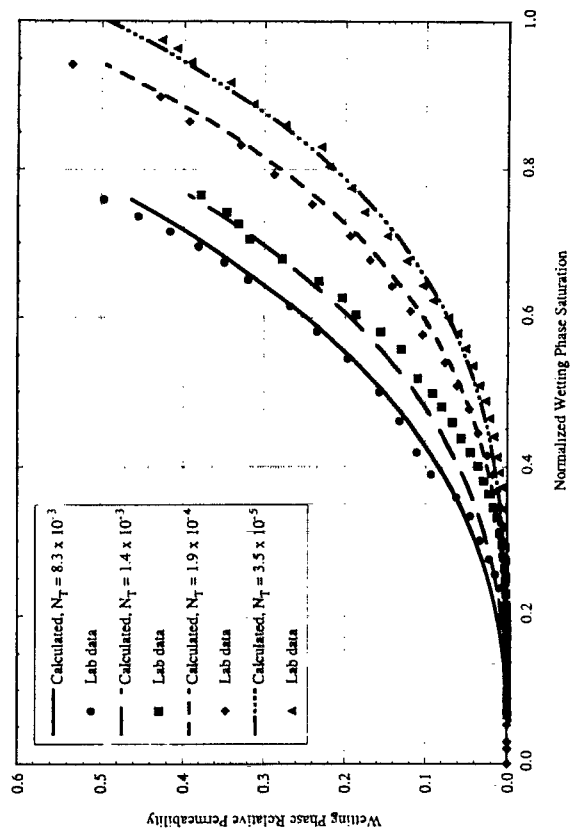


Fig. 10—Comparison of calculated and experimental wetting phase relative permeability data (Boom et al., 1996).

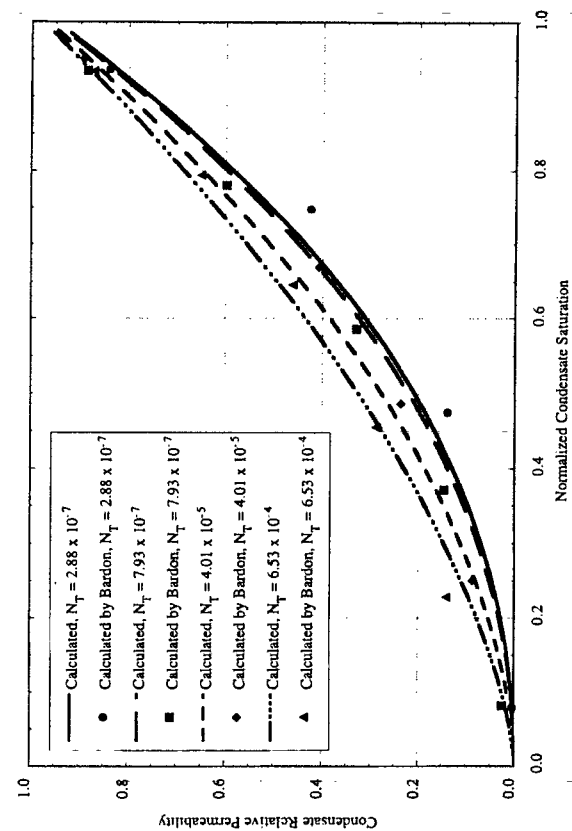


Fig. 11—Comparison of calculated and experimental condensate relative permeability data (Bardon and Longeron, 1960).

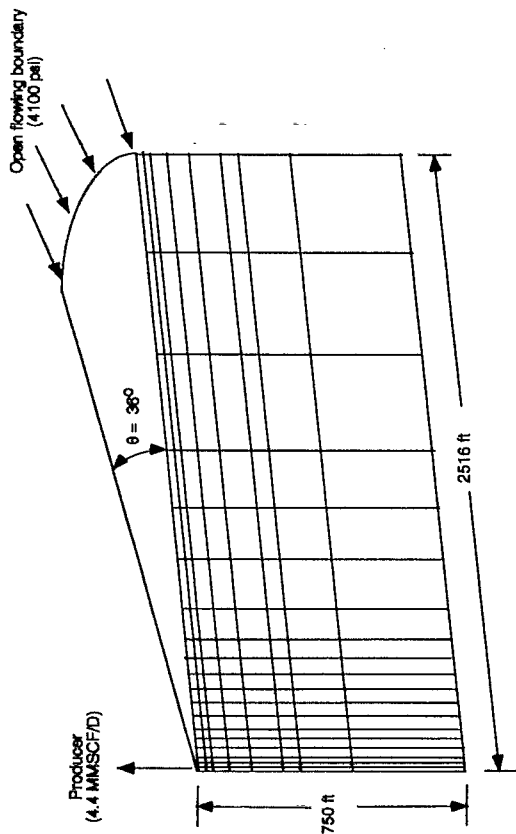


Fig. 12—Schematic of gridding scheme used in the simulation study.

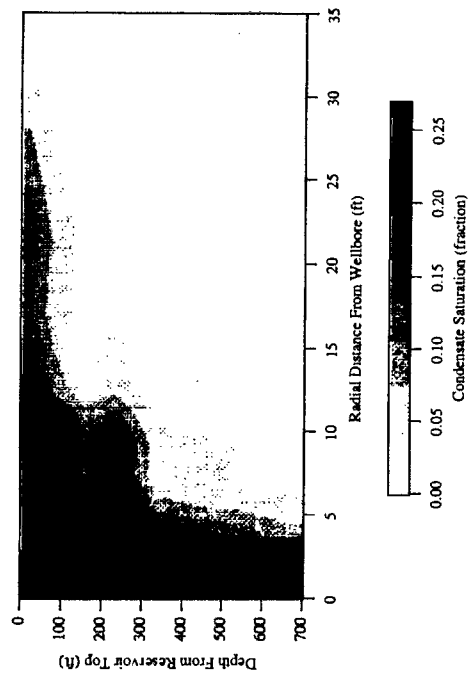


Fig. 14—Condensate saturation map at 60 days (without trapping number effects).

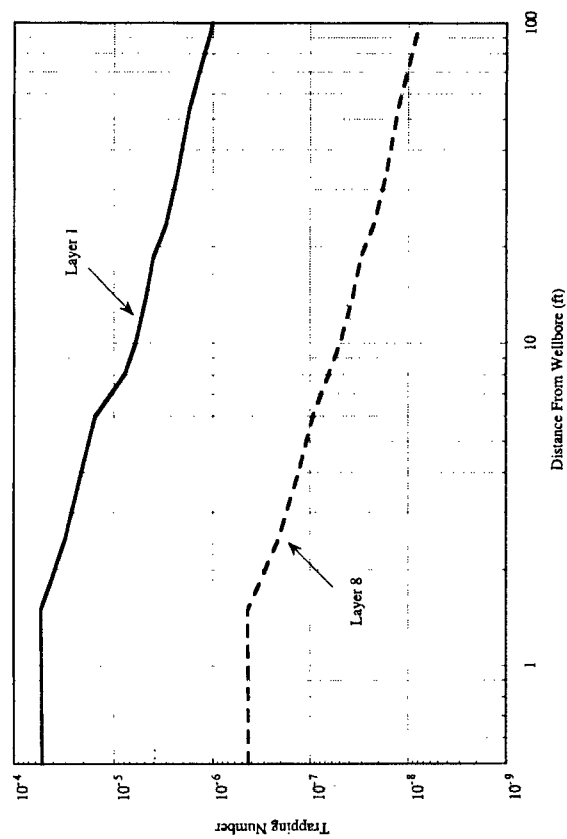


Fig. 15—Trapping number as a function of distance from the wellbore for highest and lowest permeability layers.

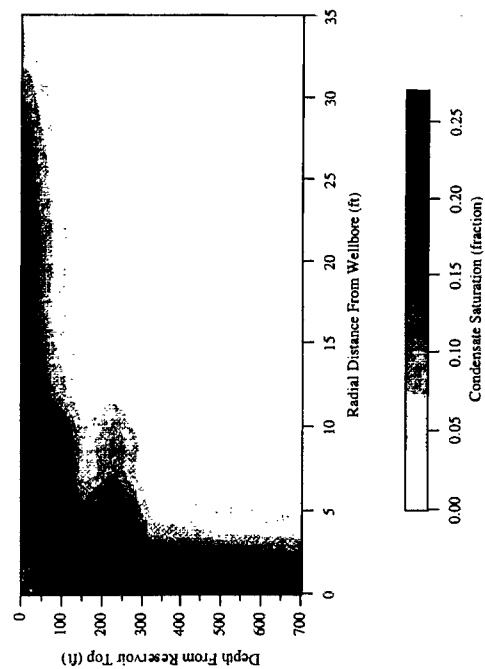


Fig. 13—Condensate saturation map at 60 days (including trapping number effects).

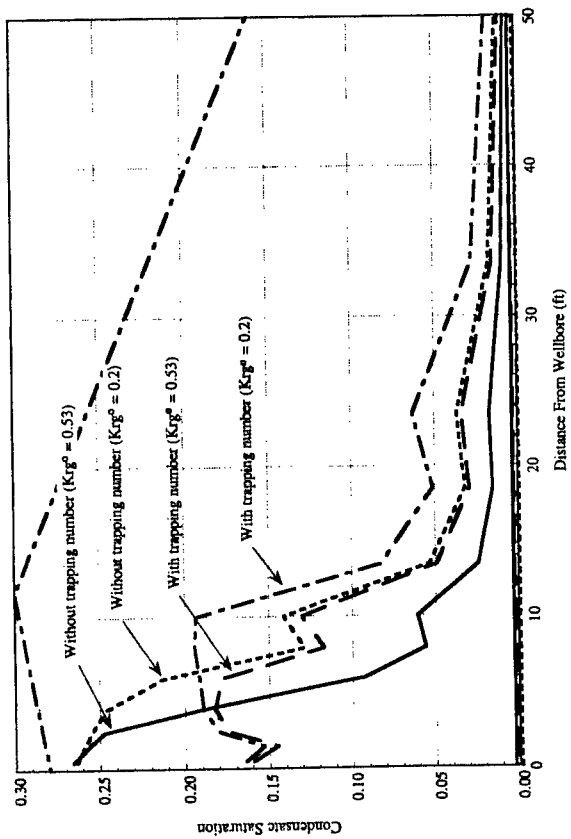


Fig. 16—Condensate saturation for layer 1.

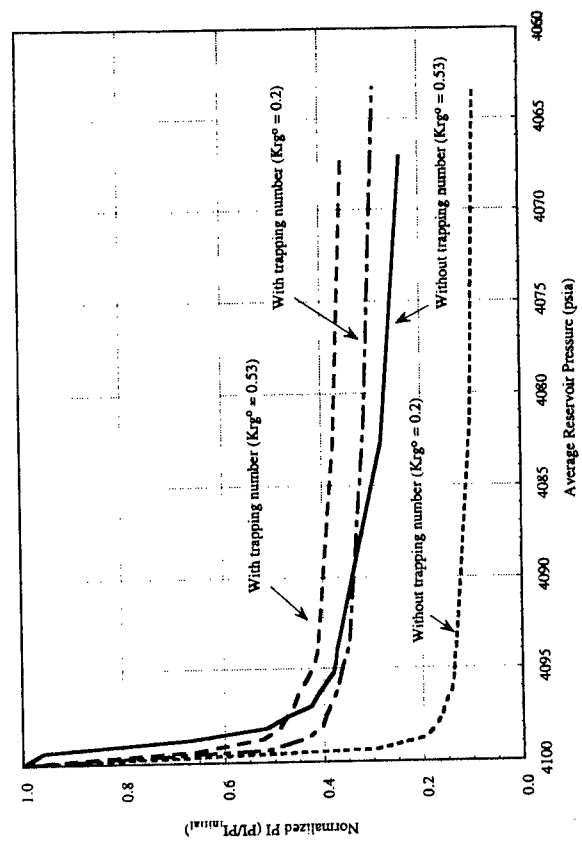


Fig. 17—Normalized productivity index.